Journal of Alloys and Compounds 692 (2017) 787–792

Contents lists available at ScienceDirect

Journal of Alloys and Compounds

journal homepage: http://www.elsevier.com/locate/jalcom

Melting temperature of $YBa_2Cu_3O_{7-x}$ and $GdBa_2Cu_3O_{7-x}$ at subatmospheric partial pressure

Fadila Taïr [a, b], Laura Carreras [a], Jaume Camps [a], Jordi Farjas [a], Pere Roura [a, *], Albert Calleja [c], Teresa Puig [d, *], Xavier Obradors [d]

[a] University of Girona, Montilivi Campus, Edif. PII, E17003 Girona, Catalonia, Spain
[b] Departement de Physique, Université des Sciences et de la Technologie d'Oran USTO, Oran, Algeria
[c] OXOLUTIA SL, Edifici Eureka, Parc de Recerca de la UAB, 08193, Bellaterra, Catalonia, Spain
[d] Institut de Ciència de Materials de Barcelona, Consejo Superior de Investigaciones Científicas (ICMAB-CSIC), Campus de la UAB, 08193 Bellaterra, Catalonia, Spain

ARTICLE INFO

Article history:
Received 26 July 2016
Accepted 9 August 2016
Available online 20 August 2016

Keywords:
High-Tc superconductors
Phase transitions
Cuprates
Thermal analysis

ABSTRACT

The melting temperature, T_m, of $YBa_2Cu_3O_{7-x}$ and $GdBa_2Cu_3O_{7-x}$ superconductor ceramic compounds has been measured by differential thermal analysis (DTA) over a large oxygen partial pressure range of five orders of magnitude ($2\cdot10^{-5} < P_{O2} < 1$ bar). It is shown that the DTA peak and endset temperatures are closer to T_m than the onset temperature. Correct measurement of T_m requires low heating rates and subatmospheric pressure conditions to avoid temperature shifts due to local oxygen overpressure and kinetic effects.

© 2016 The Authors. Published by Elsevier B.V. This is an open access article under the CC BY license (http://creativecommons.org/licenses/by/4.0/).

1. Introduction

Thermal stability of cuprate superconductor ceramic compounds, $RE_1Ba_2Cu_3O_{7-x}$ (REBCO) (RE means "rare earth"), is limited by incongruent melting at T_m, according to reaction:

$$RE_1Ba_2Cu_3O_{7-x} \rightarrow n\ RE_2BaCuO_5 + L + m\ O_2, \quad (1)$$

where L is a liquid phase. Knowledge of T_m is crucial for growing bulk superconductors from the melt [1–3] and to set the maximum processing temperature for superconductor tapes prepared by vacuum deposition techniques or from metal-organic precursor salts [4–7]. Furthermore, T_m constitutes an essential input to construct the ternary REO-BaO-CuO_{2-x} phase diagram and so to control nucleation and growth phenomena for epitaxial thin film and coated conductors preparation [6,8,9].

Among REBCO high-temperature superconductors, $YBa_2Cu_3O_{7-x}$ (YBCO) is the most extensively studied because of its high critical temperature of 92 K and because, when prepared in the form of thin film or coated conductor, it can carry high electric currents at high magnetic fields [10–12]. On the other hand, $GdBa_2Cu_3O_{7-x}$ (GdBCO), seems a good candidate to compete with YBCO. Its critical temperature is about 3 K higher [9,13], what opens the possibility of carrying higher electric currents than with YBCO.

The value of T_m of YBCO near $P_{O2} = 1$ bar has been reported by many authors [14]. They agree within a large error bar of ±10 °C. In contrast, its dependence on the oxygen partial pressure, P_{O2}, has been measured by only three authors. Lay et al. [14] determined T_m by simultaneous thermogravimetric (TG) and differential thermal analysis (DTA) experiments on powders. The results of Lindemer et al. [15] relied on TG carried out on powders and, finally, those of Kim et al. [16] were obtained on YBCO compacts by DTA. Fig. 1 summarizes these results. At first sight, the reader may be surprised by the fact that the points of Lay et al. [14] and those of Kim et al. [16] are not aligned in a $\log(P_{O2})$ vs 1000/T plot. This means that Clausius-Clapeyron equation:

$$\Delta H_m = -mR\frac{dLn(P_{O2})}{d1/T}, \quad (2)$$

(R, the gas constant and m is defined in eq. (1)) is not obeyed, or that the enthalpy of melting, ΔH_m, depends on P_{O2}.

Fig. 1 also highlights the large discrepancies between the authors. Notice that the values of Kim et al. [16] and Lay et al. [14] are

* Corresponding authors.
E-mail addresses: pere.roura@udg.cat (P. Roura), teresa@icmab.es (T. Puig).

http://dx.doi.org/10.1016/j.jallcom.2016.08.072
0925-8388/© 2016 The Authors. Published by Elsevier B.V. This is an open access article under the CC BY license (http://creativecommons.org/licenses/by/4.0/).

about 30 °C higher than those reported by Lindemer et al. [15] for $P_{O2} > 10^{-2}$ bar and this discrepancy increases at lower oxygen partial pressures. The possible reasons for these discrepancies can be classified in two categories: the YBCO melting kinetics and the local oxygen overpressure around the sample.

The reaction kinetics determines the shape of the DTA peak or the TG mas-loss step and, in particular, their onset temperature. In Fig. 2 we have plotted typical TG/DTA curves obtained from one particular experiment at $1 \cdot 10^{-2}$ bar. Since the DTA peak begins with zero slope, it is impossible to know where melting begins. So, without fitting the DTA curve to a kinetic model of the process, one cannot obtain a reliable onset temperature, T_{ONSET} (the same argument applies to the TG curve because, as seen in the inset of Fig. 2, its temperature evolution is equivalent to that of the DTA peak). Consequently, determination of T_{ONSET} is somewhat arbitrary. On the other hand, since incongruent melting involves atomic diffusion through the liquid [17], the process will be delayed to higher temperature when experiments are done at a faster heating rate [18].

The oxygen evolved during melting increases the local partial pressure at the sample pores or at the interstitial cavities. This effect will be more pronounced at lower partial pressure, for compacts than for powders, for larger samples, and for faster heating rates. All these expected dependencies are consistent with the deviations between Lay's and Kim's experimental points and with the systematic shift of these points when the nominal pressure gets lower. Thus, we wonder whether the systematic deviation of T_m below 10^{-3} bar from its linear behavior at high pressure (Fig. 1) is real or it is an experimental artifact due to local oxygen overpressure.

The experiments reported in the present paper will illustrate the effect of both the reaction kinetics and the oxygen transport out of the sample. It will be shown that T_m is closer to the endset temperature, T_{ENDSET}, or to the peak temperature T_{PEAK}, than to T_{ONSET} since melting of REBCO is not an invariant reaction. Our procedure to measure T_m will be applied to both YBCO and GdBCO. At present, the pressure dependence of T_m for GdBCO relies on two experimental points measured by Iida et al. [1].

2. Materials and methods

YBCO powders were purchased from SOLVAY (powder A) and CERACO (powder B). The metal content and stoichiometric relationship were quantified by complete dissolution in excess hot HCl(aq) acid. Y^{3+} was determined by complexometry with EDTA 0.1 M and xylenol orange as indicator at pH = 5 with acetic acid/acetate buffer and dimethylthiourea for masking the interfering Cu^{2+}. Barium content was obtained by gravimetry with an excess of potassium dichromate at pH = 5 and weighted as $BaCrO_4$ (adapted from Ref. [19]). Concentration of Cu^{2+} cation was performed by iodometry using the classical procedure of using sodium thiosulphate and starch as an indicator with addition of sodium thiocyanate for better detection of the end-point [20]. Deviations from theoretical content of Y, Ba and Cu were found below 0.6%, 1.5% and 0.3% for powder A and 0.8%, 0.5% and 2.5% for powder B. On the other hand, XRD curves revealed the presence of secondary $BaCO_3$ and CuO phases in powder A whereas all the XRD peaks of powder B could be assigned to orthorhombic YBCO (Fig. 3). The amount of $BaCO_3$ in powder A was quantified through the area of the endothermic DTA peak appearing near 810 °C that corresponds to the $BaCO_3$ polymorphic phase change [21]. We deduce that powder A contained 4.7% in weight of $BaCO_3$ or, in other words, that 14% of Ba atoms were in the carbonate phase. This DTA peak was not detectable in powder B.

GdBCO was prepared from high purity Gd_2O_3, CuO and $BaCO_3$ powders purchased from Sigma-Aldrich. After intensive mixing using a mortar and pestle, these precursors were reacted at 950 °C in air for 1 h, grinded and treated again at the same temperature for 16 h. No phases except orthorhombic GdBCO were detected by XRD.

Thermal analysis experiments were done by a simultaneous TG/DTA apparatus (Setsys evolution of Setaram). In a standard experiment, 10 mg of powder were introduced in an alumina pan (diameter ϕ = 5 mm; height H = 1.75 mm). However, different masses and pans were used to test for the local oxygen overpressure. All the experiments but one were carried out at a heating rate, β, in the 1–20 °C/min range and the recorded "sample temperature" was corrected by the apparatus thermal lag that was determined by melting a high-purity Ag reference. This calibration procedure was also done at subatmospheric conditions.

High purity N_2, O_2 and synthetic air were introduced into the apparatus furnace through a mass flowmeter. For the atmospheric pressure experiments (P_{O2} below 10^{-2} bar), P_{O2} was measured at the apparatus exit valve by a fuel cell sensor gas (OxyTrans of Roscid Technologies). The total flux was kept around 400 mL/min to ensure proper P_{O2} measurement conditions. For subatmospheric experiments, O_2 or air were introduced at the rate of 5 mL/min and the total pressure, P, was controlled with a manual valve located

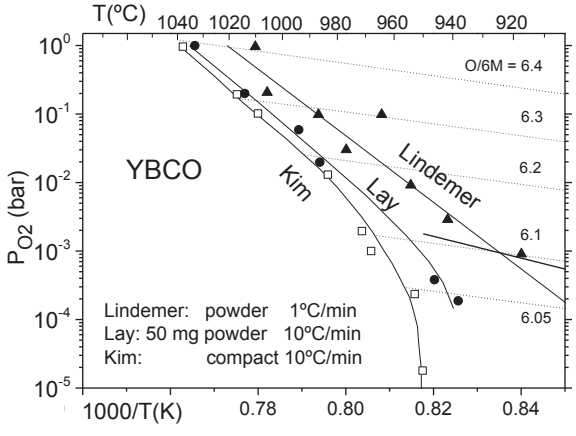

Fig. 1. Values of the YBCO melting temperature as a function of oxygen partial pressure reported by several authors [14–16]. Solid line near the bottom-right corner: low-temperature decomposition process. Dotted lines: oxygen content in YBCO, O/6 M = 7−x [15].

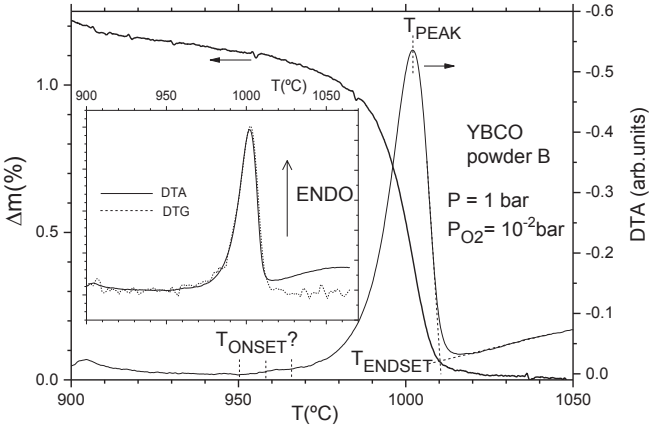

Fig. 2. Typical TG/DTA curves measured in this study. The figure highlights the difficulty to determine T_{ONSET} with accuracy. The procedure used to determine T_{ENDSET} is sketched. Inset: the derivative of the TG curve (DTG) coincides with the DTA peak.

between the furnace and a rotary pump. P was measured with a Pirani gauge.

3. Results and discussion

3.1. Onset temperature vs peak and endset temperatures

The melting of YBCO powders has been measured at 20°C/min at several oxygen partial pressures ranging from $5\cdot10^{-5}$ to 0.2 bar (air). The onset temperature of the DTA peaks has been plotted in Fig. 4. Discrepancy between powders A and B is as large as 20 °C. In contrast, if peak or endset temperatures are plotted instead (Fig. 4), much better agreement is obtained. They match within an error bar of ±3 °C. In view of the difficulty to define where the peak onset is located (Fig. 2), the discrepancy of T_{ONSET} is not surprising. Use of T_{PEAK} and T_{ENDSET} is better from a practical point of view and, for these particular samples, they seem much more reliable. In this subsection, we will also show that, when measured at the right conditions, this particular quantification of T_m is, also, more correct from a thermodynamic point of view.

One difficulty associated with T_{PEAK} (and T_{ENDSET}) is that incongruent melting involves atomic diffusion through the liquid [17] and, consequently, when it is measured out of equilibrium, as under our DTA/TG experiments, it can occur at higher temperature when β is increased. The shift of the DTA peak with β has been measured in air between 1 and 20°C/min. As expected, T_{PEAK} is minimum for 1°C/min (Fig. 5). The temperature shift with β we have measured is very similar to that reported by Plewa et al. [18]. However, since melting occurs near the equilibrium temperature, the shift of the DTA peak cannot be described like a thermal activated process governed by Arrhenius reaction rates and, consequently, the energy activation values they obtained have a doubtful meaning.

Notice that the DTA peaks of Fig. 5 evolve in such a way that one would not expect any significant shift if the heating rate were further reduced. To verify this prediction, the analysis must rely on the mass-loss TG curves, because at lower heating rates the DTA signal becomes very weak. The coincidence of curves measured at 1 and 0.2°C/min (inset of Fig. 5) means that the sample has not a single melting point but that it melts over a temperature range. In other words, the smooth onset of the DTA peak and peak width are not due to any kinetic effect or to any broadening related to the experimental technique. If the sample is held at, say, 1025 °C only half of its mass will melt. To reach complete melting, temperature must be further raised.

The existence of a melting range means that melting of YBCO is not an invariant reaction. Of course, this conclusion agrees with the Gibbs rule of phases:

$$F = C - P + 2, \tag{3}$$

where the number of components, C, is 4 (Y_2O_3, BaO, CuO and O), and the number of coexisting phases, P, is 4 (Eq. (1)). So, during melting, the state of equilibrium has two degrees of freedom (F = 2). Once P_{O2} is set through the furnace atmosphere, the temperature can still vary during melting.

Sometimes, the reaction of Eq. (1) is known as "peritectic melting" of YBCO. This is not strange because, similarly to the peritectic melting in binary systems, the reaction products are one solid and one liquid phase. However, the reader should not be confounded by the fact that, according to Gibb's rule of phases, for binary systems peritectic melting is an invariant reaction. As a consequence, peritectic melting of binary alloys have well defined onset temperatures (as in Cu-Ge alloys [22]) whereas, for ternary or quaternary systems the onset may be ill-defined (as for $SrBi_2B_4O_{10}$ [23]), depending on the number of coexisting phases. The quaternary Y_2O_3-BaO-CuO-O system has its own peritectic point corresponding to reaction [14,15]:

$$a\ Y_1Ba_2Cu_3O_{7-x} + b\ CuO \rightarrow c\ Y_2Ba_1Cu_1O_5 + L + d\ O_2 \tag{4}$$

with a/b = 7/3, that is invariant at constant P_{O2}. For these reasons, we prefer to refer reaction of Eq. (1) simply as "YBCO melting".

In contrast with invariant melting, like that occurring at the eutectic or peritectic points of a binary alloy, for non-invariant melting, T_{ONSET} is not the good experimental parameter to quantify the melting point. Since representation of ternary of quaternary phase diagrams is very difficult, we will illustrate the status of T_{ONSET} with the binary phase diagram of Fig. 6. Deviation from eutectic composition, x_E, (whose melting is invariant) keeps unchanged the onset temperature of the DTA peak, however, deviation from the intermetallic concentration, x_0, (whose melting in non-invariant) lowers the peak onset. Fig. 6 makes also clear that, for non-invariant melting, T_{PEAK} is closer to the melting point than T_{ONSET} is. In fact, we must conclude that, in the absence of any

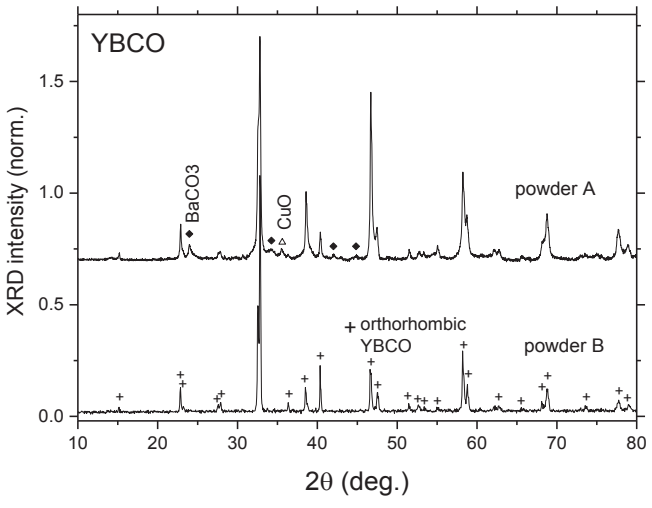

Fig. 3. Powder XRD curves showing that secondary phases have been only detected in YBCO powder A.

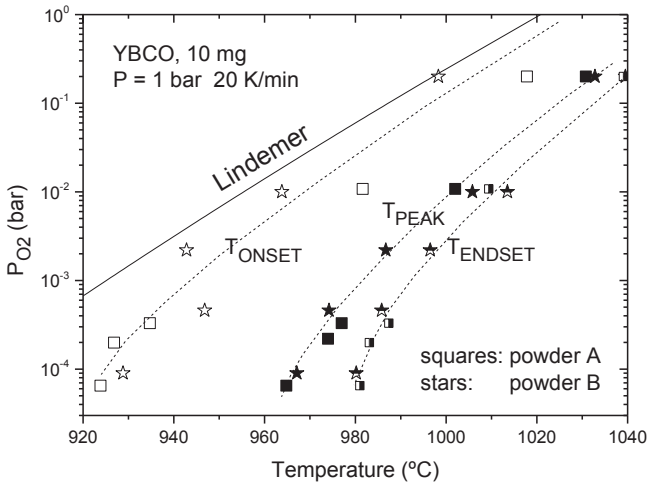

Fig. 4. Summary of our results obtained at atmospheric total pressure. T_{PEAK} and T_{ENDSET} values show a much lower dispersion than T_{ONSET}. For comparison, the dependence found by Lindemer et al. [15] is also plotted.

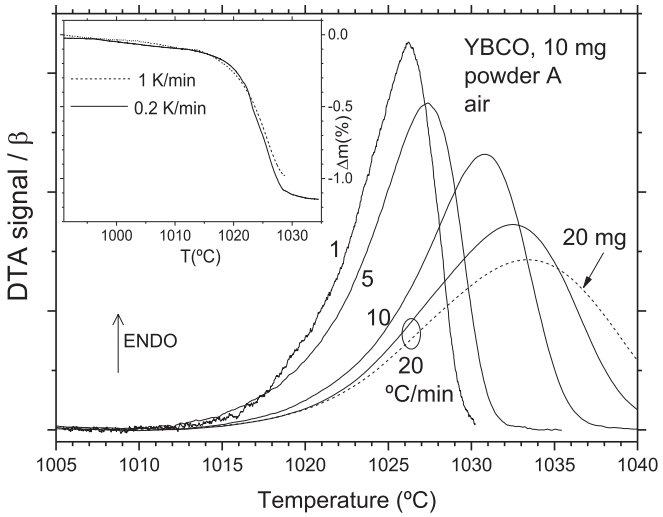

Fig. 5. DTA peaks measured in air to show the important effect of the melting kinetics and the minor effect of sample mass. Inset: comparison of TG curves measured at 1°C/min and 0.2°C/min indicating that, at 1°C/min, kinetic effects on the peak shape are negligible.

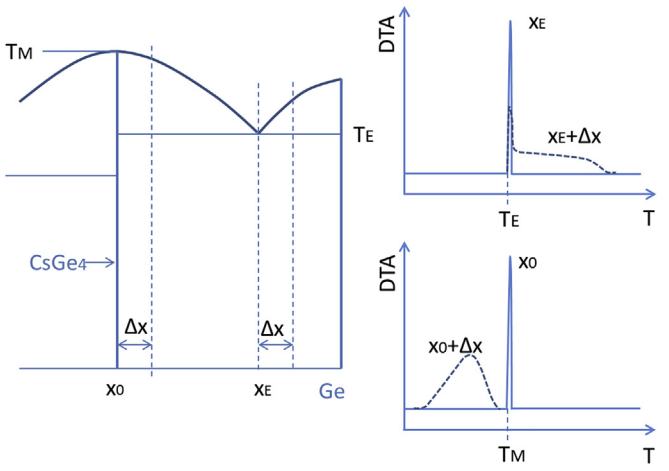

Fig. 6. The effect on the melting peak shape of deviation Δx from the composition of a stoichiometric compound, $CsGe_4$ (non-invariant reaction) and a eutectic alloy (invariant reaction). Deviation from the stoichiometric composition (lower DTA figure) broadens and shifts the DTA peak to lower temperature, whereas the DTA onset does not change for deviations around the eutectic composition (upper DTA figure).

kinetic effect, T_{ENDSET} is even closer to the melting point.

This analysis also applies to the YBCO melting. In fact, the pseudobinary section of the ternary Y_2O_3-BaO-CuO diagram going from YBCO to CuO [15] clearly shows that below its melting point, YBCO can coexist with a liquid phase, like the stoichiometric compound of Fig. 6. If one YBCO sample had exactly the 1/2/3 = Y/Ba/Cu ratio, then it would melt at a well-defined temperature (like one sample with the intermetallic composition x_0 of Fig. 6). However, the observed melting range tells us that this condition is not fulfilled in our samples and, probably, this is also the case for the results of Fig. 1. Consequently, T_{PEAK} and T_{ENDSET} are always a lower bound of T_m. In contrast, the points of Lindemer et al. [15] and Kim et al. [16] were obtained from the onset of TG and DTA experiments, respectively. Probably this is also the case of the points of Lay et al. [14] because this is the usual criterion used to determine by DTA the melting point of pure substances.

3.2. Oxygen local overpressure

Although, all along this section, we discuss the evolution of T_{PEAK}, the results are also valid for T_{ENDSET}.

During melting, O_2 evolves from the YBCO sample. Its out-diffusion will give rise to oxygen overpressure that can shift the process to higher temperature. Since overpressure is proportional to the oxygen flux out of the crucible, it will be higher for larger samples, higher heating rates and taller crucibles. At constant total pressure (in our present experiments, P = 1 bar), its effect on DTA peak shift will be negligible in air or in pure oxygen whereas it may be very important at low P_{O2}. On the other hand, the effect on the peak onset will be smaller than on its peak temperature because, although oxygen also evolves due to equilibration with the furnace atmosphere before melting [14,24] (see the small slope before of the TG curve before the mass-loss step, in Fig. 2), the oxygen flux is much smaller.

All these dependencies are clearly illustrated in Fig. 7. For 10 mg, T_{PEAK} shifts +7 °C when β is increased from 5 to 10°C/min at $65\cdot10^{-6}$ bar. This shift cannot be explained by the kinetic dependence discussed above (Fig. 5) that would account for only 3 °C. Concerning the sample mass, when it passes from 10 to 20 mg, the DTA peak measured at 20°C/min is shifted by more than 15 °C that should be compared to the small shift of 1 °C in air (Fig. 5). And, finally, a tall crucible (H = 5 mm, ϕ = 3.9 mm) with a large mass of 50 mg exhibits an additional peak shift of 30 °C. Concerning the peak onset, one cannot assess any systematic shift from Fig. 7. This behavior of the onset agrees with the experiments carried out by Lindemer et al. to test for the effect of oxygen overpressure [15].

The excess oxygen concentration, ΔC_0, can be approximately calculated by considering that oxygen transport is governed by molecular diffusion and that, at the top of the crucible, there is no oxygen overpressure, i.e.:

$$\Delta C_0 = \frac{F \cdot H}{D}, \tag{5}$$

where D is the oxygen diffusivity in air ($8.1\ 10^{-5}$ m^2/s at 1 bar and 950 °C [25]), and F is the flux of oxygen that can be easily determined from the TG curve by assuming that the mass-loss is due to oxygen. Application of Eq. (5) to the standard experiment (H = 1.75 mm, ϕ = 5 mm, 10°C/min) delivers an overpressure of $3\cdot10^{-3}$ bar, more than one order of magnitude higher than the nominal partial pressure ($6.5\cdot10^{-5}$ bar).

3.3. Dependence of T_m on P_{O2}

The previous subsections have made clear that T_{ONSET} is not the good parameter to quantify T_m and that T_{PEAK} or T_{ENDSET} should be used instead. Furthermore, since the DTA peak shifts due to melting kinetics and oxygen overpressure, experiments must be designed to avoid these parasitic effects. As shown in Fig. 5, a heating rate of 1°C/min is slow enough to prevent any kinetic effect. However, even at this slow heating rate, oxygen overpressure would be too high (about $0.3\ 10^{-3}$ bar) for measuring correct peaks below 10^{-3} bar. So, except for air and oxygen, all experiments have been done at sub-atmospheric pressure ($P = P_{O2}$). At these conditions, oxygen overpressure will be negligible, since gas diffusivity (D in Eq. (5)) is proportional to 1/P [25].

The melting of YBCO and GdBCO has been measured at P_{O2} values ranging from 1 to $2\cdot10^{-5}$ bar. To avoid any kinetic effect, a heating rate of 1°C/min was programmed. At these conditions, all experiments delivered a single DTA peak (Fig. 8) except for the lowest pressure where no DTA/TG signal could be measured. This is because, below $2\cdot10^{-3}$ bar, YBCO [15] decomposes through a slower

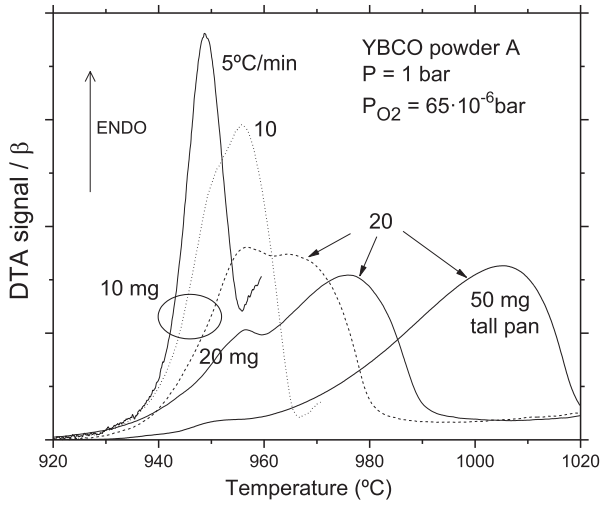

Fig. 7. DTA peaks measured at atmospheric pressure and $P_{O2} = 65 \cdot 10^{-6}$ bar. All of them have different shapes because of oxygen overpressure near the sample.

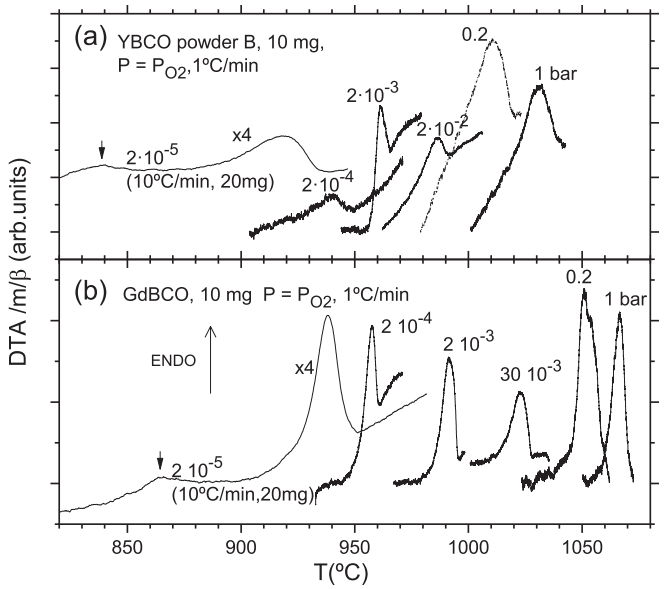

Fig. 8. DTA peaks of melting measured at several oxygen total pressures (P = P_{O2} except for air): a) YBCO, b) GdBCO. Arrows point to DTA peaks related to partial decomposition before melting.

process before T_m is reached. The equilibrium temperature of this decomposition, T_D, is plotted as a solid line in Fig. 1. At $2 \cdot 10^{-5}$ bar, T_m-T_D is so large that, at 1ºC/min, YBCO is completely decomposed before the sample reaches T_m. At $2 \cdot 10^{-4}$ bar T_m-T_D is smaller and a fraction of the initial YBCO phase survives in an unstable state until it reaches its melting point. A similar situation is encountered with GdBCO but, in this case, the low-temperature decomposition process occurs below $5 \cdot 10^{-4}$ bar [26].

To measure melting at $2 \cdot 10^{-5}$ bar, a heating rate of 10ºC/min was used. Now, the corresponding DTA peak is clearly seen (Fig. 8) and it is preceded by another exothermic process that corresponds to the low-temperature decomposition. Since, at this heating rate, a kinetic effect is expected, we consider that the T_{PEAK} and T_{ENDSET} values are shifted by 4 °C, like in air (Fig. 5).

From the DTA curves of Fig. 8, we have extracted the T_{PEAK} and T_{ENDSET} values collected in Fig. 9. As already commented on in Section 3.1, we consider that they are a lower bound to T_m. We can now compare them to the literature. First of all, we see that our values for YBCO are always higher than those published by Lindemer et al. [15], and higher than those of Lay et al. [14] and Kim et al. [16] in the $1 < P_{O2} < 10^{-2}$ bar range (Fig. 1). Of course this is expected because they took T_{ONSET} as T_m. A similar deviation is observed for GdBCO [1] (Fig. 9). If Lindemer's curve is taken as a reference (as done by most authors), our results deliver a value of T_m that is 15 or 40 °C higher at $P_{O2} = 1$ and 10^{-4} bar, respectively.

Concerning the dependence on P_{O2}, our results suggest that the systematic deviations of T_m to higher temperatures for P_{O2} below 10^{-3} bar reported by Lay et al. [14] and Kim et al. [16] were due to local oxygen overpressure. Furthermore, the dependence of T_m on P_{O2} is smoother than that reported by Lindemer et al. [15] and Iida et al. [1] for YBCO and GdBCO, respectively. Our points agree with Clausius-Clapeyron equation (Eq. (2)) and, consequently, they can be linearly fitted to:

$$\log(P_{O2}(bar)) = 49.9(16) - 65.4(20) \cdot \frac{1000}{T_{ENDSET}(K)} \quad \text{for YBCO} \tag{6}$$

and

$$\log(P_{O2}(bar)) = 40.8(16) - 55.0(20) \cdot \frac{1000}{T_{ENDSET}(K)} \quad \text{for GdBCO,} \tag{7}$$

where we consider that T_{ENDSET} is the value closest to T_m. In Fig. 1 the oxygen content of YBCO is indicated. For these low values of x ($x < 0.2$), YBCO is always tetragonal [24]. And the same can be said for our GdBCO experiments [27]. Transition to the orthorhombic phase only occurs at a much lower temperature and, consequently, it has no influence on our results.

Finally, application of Clausius-Clapeyron Eq. (2) allows us to calculate the enthalpy and entropy variation:

$$\Delta S_m = \Delta H_m / T_m \tag{8}$$

during melting. The value of m (Eq. (2)) can be directly extracted from the TG mass-loss step. In air, we have obtained $m = 0.210$ and 0.168 for YBCO and GdBCO, respectively. These values lead to $\Delta H_m = 264$ and 177 kJ/mol and to $\Delta S_m = 206$ and 134 J/K/mol, for YBCO and GdBCO, respectively.

4. Conclusions

In contrast with binary systems, melting of REBCO is not an invariant reaction. Therefore, unless the metal ratio of samples is exactly 1/2/3 and no extra phases coexist with REBCO, melting occurs over a temperature range. As a consequence, T_m is better determined by T_{PEAK} and T_{ENDSET} than T_{ONSET}. Furthermore, the onset temperature is difficult to determine from experiment because the melting peak begins with zero slope. As a result, T_{ENDSET} and T_{PEAK} are more reliable than T_{ONSET} from both theoretical and practical points of view.

The problem with T_{PEAK} and T_{ENDSET} is that, due to kinetic effects and oxygen local overpressure, the DTA peak tends to be shifted to higher temperature. The kinetic effect can be avoided by programming the experiments at a low heating rate of 1ºC/min. Although local overpressure is reduced at this heating rate, it is still too high for measuring T_m below 10^{-3} bar. So, we have decided to

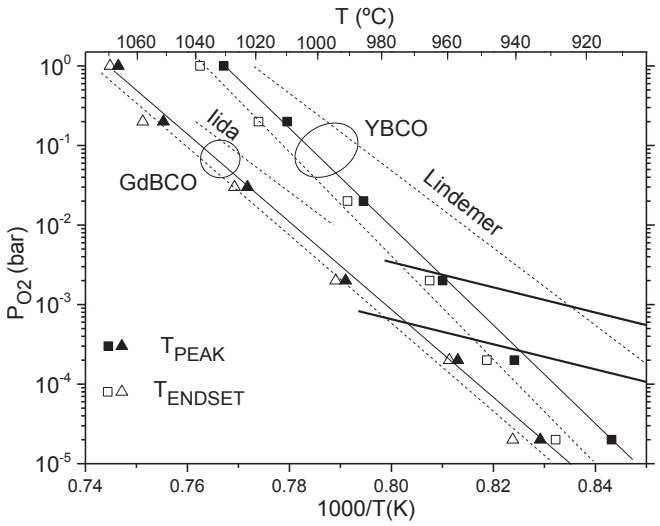

Fig. 9. Peak and onset temperatures obtained from DTA experiments at $P = P_{O2}$ for YBCO and GdBCO powders are compared to the values found in the literature [1,15]. Our values have to be considered as a lower bound to melting temperature, T_m. The lines at the bottom-right corner are the equilibrium temperatures of a low-temperature decomposition process.

carry out the experiments at subatmospheric conditions ($P = P_{O2}$).

All these precautions have allowed us to quantify T_m of YBCO and GdBCO over a variation of P_{O2} of five orders of magnitude ($2 \cdot 10^{-5} < P_{O2} < 1$ bar). The dependence of T_m on P_{O2} follows the Clausius-Clapeyron equation with constant melting enthalpies of 264 and 177 kJ/mol for YBCO and GdBCO, respectively. This dependence is maintained down to the lowest oxygen partial pressure, where YBCO and GdBCO reach T_m after partial decomposition. With regard to accuracy and P_{O2} range, our results represent a significant improvement in the determination of T_m for YBCO and GdBCO with respect to the values already published in the literature.

Acknowledgments

This work was funded by the Spanish Programa Nacional de Materiales through projects MAT2014-51778-C2-1-R and MAT2014-51778-C2-2-R. We also acknowledge: the Center of Excellence award Severo Ochoa SEV-2015-0496, SGR753 and SGR948 from the Generalitat of Cataluny, the European Union through projects Eurotapes (EU-FP7 NMP-LA-2012-280432) and Ultrasupertape (ERC ADG-2014-669504), and the Universitat de Girona (MPCUdG2016/059). FT acknowledges financial support from USTO. The authors are indebted to Dr. Joan Pere López Olmedo and Dr. Xavier Fontrodona of STR, University of Girona, for their technical assistance.

References

[1] K. Iida, N.H. Baber, Y. Shi, D.A. Cardwell, Supercond. Sci. Technol. 19 (2006) S478–S485.
[2] X. Obradors, R. Yu, F. Sandiumenge, B. Martinez, N. Vilalta, V. Gomis, T. Puig, S. Piñol, Supercond. Sci. Technol. 10 (1997) 884–890.
[3] M. Murakami, N. Sakai, T. Higuchi, S. Yoo, Supercond. Sci. Technol. 9 (1996) 1015–1032.
[4] R. Feenstra, T.B. Lindemer, J.D. Budai, M.D. Galloway, J. Appl. Phys. 69 (1991) 6569–6585.
[5] X. Obradors, T. Puig, A. Pomar, F. Sandiumenge, N. Mestres, M. Coll, A. Cavallaro, N. Roma, J. Gazquez, J.C. Gonzalez, O. Castano, J. Gutierrez, A. Palau, K. Zalamova, S. Morlens, A. Hassini, M. Gibert, S. Ricart, J.M. Moreto, S. Pinol, D. Isfort, J. Bock, Supercond. Sci. Technol. 19 (2006) S13–S26.
[6] X. Obradors, T. Puig, S. Ricart, M. Coll, J. Gazquez, A. Palau, X. Granados, Supercond. Sci. Technol. 25 (2012) 123001.
[7] P. Wermeir, J. Feys, J. Schaubroeck, K. Verbeken, P. Lommens, I. Driesche, Mater. Res. Bull. 47 (2012) 4376–4382.
[8] J. Gazquez, F. Sandiumenge, M. Coll, A. Pomar, N. Mestres, T. Puig, X. Obradors, Y. Kihn, M.J. Casanove, C. Ballesteros, Chem. Mater. 18 (2006) 6211–6219.
[9] Jae-Hun Lee, Hunju Lee, Jung-Woo Lee, Soon-Mi Choi, Sang-Im Yoo, Seung-Hyun Moon, Supercond. Sci. Technol. 27 (2014) 044018.
[10] A. Gurevich, Nat. Mater. 10 (2011) 255–259.
[11] D. Larbalestier, A. Gurevich, D.M. Feldmann, A. Polyanskii, Nature 414 (2001) 368–377.
[12] X. Obradors, T. Puig, Supercond. Sci. Technol. 27 (2014) 044003.
[13] L.H. Jin, Y.F. Lu, W.W. Yan, Z.M. Yu, Y. Wang, C.S. Li, J. Alloys Comp. 509 (2011) 3353–3356.
[14] K.W. Lay, G.M. Renlund, J. Am. Ceram. Soc. 73 (1990) 1208–1213.
[15] T.B. Lindemer, F.A. Washburn, C.S. MacDougall, R. Feenstra, O.B. Cavin, Phys. C 178 (1991) 93–104.
[16] J. Kim, D. Gaskell, J. Am. Ceram. Soc. 77 (1994) 753–758.
[17] E.A. Brener, D.E. Temkin, Acta Mater. 55 (2007) 2785–2789.
[18] J. Plewa, H. Altenburg, J. Opfermann, J. Therm. Anal. 47 (1996) 379–390.
[19] M.A. Malati, Experimental Inorganic/Physical Chemistry: an Investigative, Integrated Approach to Practical Project Work, Woodhead Publishing Ltd., Oxford, 2010, p. p.59.
[20] J. Mendham, R.C. Denney, J.D. Barnes, M.J.K. Thomas, Vogel's Quantitative Chemical Analysis, sixth ed., Longman Group Ltd., London, 1979, p. 393.
[21] R. Strobel, M. Maciejewski, S.E. Pratsinis, A. Baiker, Thermochim. Acta 445 (2006) 23–26.
[22] W. Zhai, D.L. Geng, W.L. Wang, B. Wei, J. Alloys Comp. 535 (2012) 70–77.
[23] M.G. Krzhizhanovskaya, R.S. Bubnova, A.V. Egorysheva, M.S. Kozin, V.D. Volodin, S.K. Filatov, J. Solid State Chem. 182 (2009) 1260–1264.
[24] T.B. Lindemer, J.F. Hunley, J.E. Gates, A.L. Sutton Jr., J. Brynestad, C.R. Hubbard, P.K. Gallaguer, J. Am. Ceram. Soc. 72 (1989) 1775–1788.
[25] J.R. Welty, C.E. Wicks, R.E. Wilson, G. Rorrer, Fundamentals of Momentum, Heat, and Mass Transfer, Wiley, 2001.
[26] J.-W. Lee, S.-M. Choi, J.-H. Song, J.-H. Lee, S.-H. Moon, S.-I. Yoo, J. Alloy Comp. 602 (2014) 78–86.
[27] F. Prado, A. Caneiro, A. Serquis, Phys. C 295 (1998) 235–246.